Intelligent Control of Electric Scooters

D.T. Lee*
S.J. Shiah
C.M. Lee
Institute of Information Science
Academia Sinica
Taipei, Taiwan
email:{dtlee,bioman,cmlee}@iis.sinica.edu.tw

C. H. Wu
Department of Electrical and Computer Engineering
Northwestern University
Evanston, IL 60208
email: chwu@ece.northwestern.edu

ABSTRACT
Most of the present day electric scooters are equipped with a voltage-driven DC motor powered by four 12-volt lead-acid batteries and a hand-lever accelerator operated by the rider to control their speed. Because of the nonlinear battery discharge characteristics and different driving behaviors of riders, it is not easy to tell how much electric power remaining in the battery and how far the electric scooter can travel before the battery has to be re-charged. As a result, the reliability of the electric scooter is lacking.

To tackle this problem and to enhance the capabilities of present electric scooters, we propose an intelligent control system that not only can control the speed of the electric scooter, but also can provide information about residual electric power in the battery system by monitoring its power consumption.

This system consists of both motor driver control and energy management subsystems. The driver control subsystem is implemented as a closed-loop speed control system by using a muscle-like control law with excellent compliant property. The energy management subsystem is implemented by learning modules based on fuzzy neural networks and cerebellar model articulation controller networks, which can estimate and predict nonlinear characteristics of the power consumption of batteries and electric scooter dynamics. With this battery power monitoring subsystem the rider will be provided information regarding an estimated traveling distance at a given speed, and the maximum allowable speed to guarantee safety arrival at the destination with the residual battery capacity.

Experimental results show that the performance of electric scooters can be improved substantially.

KEY WORDS
Electric Scooter, Intelligent Control, Muscle-like Compliant Control, Fuzzy Neural Network, Cerebellar Model Articulation Controller

1 Introduction

There are more than ten million gasoline powered scooters or motorcycles being used in Taiwan every day. They have become a very common transportation means for people to commute to and from work. However, the amount of exhaust and noxious particles produced by the scooter is quite significant that the scooter is considered a moving air and noise pollutant and is affecting the air quality and living environment seriously[1].

In an effort to reduce air pollution, Taiwan government has implemented a subsidiary program to encourage research and development of battery powered electric scooters since 1997. However, commercially available electric scooters to date have some drawbacks, including high cost, long battery recharging time, relatively short traveling distance for each re-charge, and inadequate feedback information to the user with respect to the residual battery power. The lack of a more reliable or accurate power prediction and management mechanism often results in situations that the riders unwittingly run out of battery power before they reach their destinations or a facility to recharge the battery. This uncertainty as to when the battery power will run out, could be rather troublesome and therefore hinder the sale of electric scooters. The crux in getting a good estimate of the present battery state-of-charge (SOC) lies in the nonlinear battery discharge characteristics which vary with the road condition and the driving behavior of the rider.

To tackle the reliability problem of present electric scooters, we propose an intelligent system which consists of a motor driver control subsystem and an energy management subsystem for controlling and monitoring power consumption of electric scooters. The motor driver control subsystem (DCS) provides a closed-loop speed control and is implemented by using a muscle-like control law[2]. Its excellent compliant and short-range enhancement property can give the rider the needed feeling of acceleration and maneuverability. In contrast with the open-loop control adopted by the present electric scooters, the closed-loop control enables the rider to fully control the speed of the electric scooter. In so doing, the rider can control the consumption of electric power via the proposed subsystem. The energy management subsystem (EMS) will provide the rider with the critical information including estimated allowable traveling distance, safe speed, and remaining battery capacity etc., such that the rider can control the speed of the scooter within a proper range via DCS and en-

sure that the scooter can arrive at the destination safely. We use learning modules which consist of fuzzy neural networks (FNN)[3] and cerebellar model articulation controllers (CMAC) [4, 5] to estimate nonlinear characteristics of the power consumption of batteries and electric scooter dynamics. Online learning about power consumption is a unique feature of our EMS. It is incorporated into this subsystem to make it more adaptable to different electric scooters and driving behaviors.

2 System Implementation

The conceptual organization of the proposed intelligent control system is shown in Fig.1. As stated earlier, this system consists of two subsystems, and they are motor driver

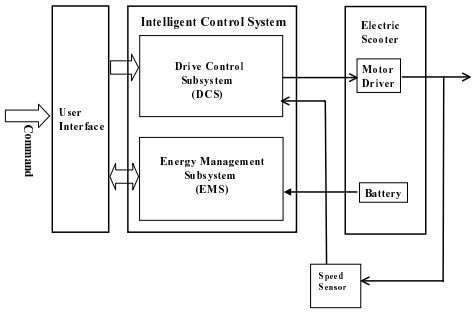

Figure 1. An illustration of the proposed intelligent control system

control subsystem (DCS) and energy management subsystem (EMS). The rider sends speed commands to DCS through a user interface which could be a lever, button, or a touch pad, and the commands will be converted into proper signals obtained from the muscle-like control law to drive the electric scooter according to the feedback velocity signals. The signal can drive the scooter to move as fast as it could to the extent as if it were operated under an open-loop control, so the rider does not have to change driving behavior. The muscle-like control also possesses a capability to filter out noisy or high-frequency disturbance input signals. It lets the scooter react to speed commands even the road condition changes constantly. On the other hand, the energy management system (EMS) monitors the power consumption of batteries and by learning the battery discharge characteristics, computes the maximum travel distance and safe speed, and provides this important information to the rider through a user interface. When the rider gets the important information, he/she will be able to make adjustments to the speed of the scooter by using DCS.
The details of these two subsystems will be discussed in the following sections.

2.1 Drive Control Subsystem(DCS)

Inspired by the compliant capabilities of the biological limb, an active damping control based on a muscle-like compliant control is adopted and implemented in the kernel motor-control subsystem for controlling an electric scooter. The proposed muscle-like control model was fitted from the responses of voluntary and involuntary limb movements[6, 7, 8, 9]. Because of its compliant adaptability, the controller is very well suited for man-machine interface control[2], such as the hand accelerator in an electric motorcycle or the foot accelerator in an electric vehicle. Because of its unique nonlinear damping property, the muscle-like control enables an electric scooter to adapt to varying loads and sudden impacting forces. The main difference between the proposed controller and the conventional controller currently used by commercially available electric scooters is that the former is a closed-loop, compliant controller while the latter is an open-loop controller. Furthermore, it can provide the rider with the feeling of great acceleration just like the open-loop control, and with cruise control capability by allowing a desirable speed to be set and maintained by DCS. The cruise control function may be disabled manually or automatically when the brake of the electric scooter is applied. Thus, the current or electric energy consumed by manual acceleration and deceleration operations can be reduced, and the life of the battery or traveling distance can be prolonged. The muscle-like compliant control model consists of two major parts: spindle-like mechanism emulating the reflex property of biological muscular system for absorbing impacting forces, and muscle-stiffness mechanism emulating muscle stiffness for tracking various movements. The control blocks of the DCS are shown in Fig.2. Both inputs of DSC are the veloc-

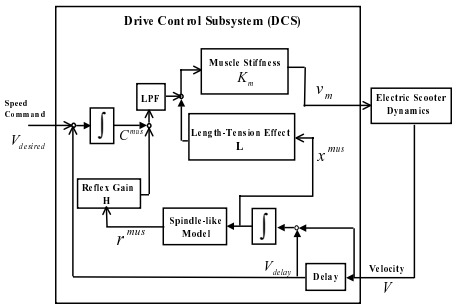

Figure 2. An illustration of the Drive Control Subsystem

ity command V_d and the feedback velocity signal V. The motor command C^{mus} used in muscle-like model is defined as

$$C^{mus} = \int (V_{delay} - V_{desire})dt \qquad (1)$$

The reflex signal of the spindle-like model, r^{mus}, scaled through a reflex gain coefficient, H, is combined with the motor command to produce a reflex-induced command for muscle force. The linear feedback gain L represents the effect of muscle length-tension which will vary with load position. Any change in muscle length will produce a muscle force through muscle stiffness K_m. The muscle force used in the present implementation of DCS is defined as the DC motor control voltage v_m. It can also be defined as the DC motor control current, depending on the type of DC motor driver used. Thus, the control law for generating v_m can be expressed as

$$v_m = K_m(Lx^{mus} + LPF(Hr^{mus} - C^{mus})) \quad (2)$$

where $LPF(\cdot)$ represents a low pass filter. The spindle-like model with the nonlinear, fractional, damping effect multiplied by the short-range elasticity enhancement cab be expressed as

$$\begin{aligned} B_p \dot{x}_p^{\frac{1}{n}}(|x_p| - x_{p0}) &= K_r(x^{mus} - x_p) \\ &= r^{mus} \end{aligned} \quad (3)$$

where x_p, $\dot{x}_p$, and x_{p0} are the internal position, velocity, and bias position of the spindle model, n is an odd integer (n=5 in our case), B_p is a damping coefficient, and K_r is the reflex stiffness. The muscle equilibrium position x^{mus} used in DCS is expressed as

$$x^{mus} = \int (V_{delay} - V)dt \quad (4)$$

where V_{delay} and V are scooter velocities at the kth and $(k+1)$st sampling times, respectively. According to Eq.(3), any reflex signal will induce a corresponding force to respond to a change of scooter velocity. This nonlinear damping can deal with disturbance variations within a large range, and reduce the effect of parameter variation of a nonlinear system.

2.2 Energy Management Subsystem(EMS)

The proposed energy management subsystem possesses functions of battery SOC prediction, battery state of health (SOH) prediction, maxmium travel distance estimation, and safe speed estimation. The performance of this subsystem depends on whether we can find a suitable method or mechanism to model the nonlinear battery charge and discharge dynamics. Learning controllers which are biologically inspired and intended to model human experience [10, 11, 12] are an attractive alternative to dealing with nonlinear systems of incomplete models or inaccurate model parameters. We therefore decide to use FNNs and CMAC networks [13] as the core of this subsystem.

In general, the battery capacity is a nonlinear function of discharge current, temperature, depth of discharge, and recharging times. At present, there are many methods for estimating the SOC, and they can be classified as load voltage method[14, 15], ampere hour accumulation method[16, 17, 18], and internal resistance method[19]. The load voltage method is suitable for constant load current applications. For electric soccters, it cannot provide precise estimations, because the load current will vary a lot with the road condition, and the load and speed change of the scooter. The ampere hour accumulation method is used to accumulate the discharge current, and estimate the SOC according to this accumulated value and pre-recorded data describing the relations between battery discharge current, voltage, and capacity. The pre-recorded data is not valid in every discharge condition, so methods making use of models of fixed parameters to estimate SOC will suffer from loss of precision when the discharge conditions are changing over time. The internal resistance method needs to measure the frequency response of the battery to determine its SOC. Because it needs extra electric circuits and function generators, it is difficult to implement.

In our EMS, we use four learning modules, as shown in Fig.3. These four learning modules are implemented with FNNs and CMAC networks, as shown in Fig. 4.

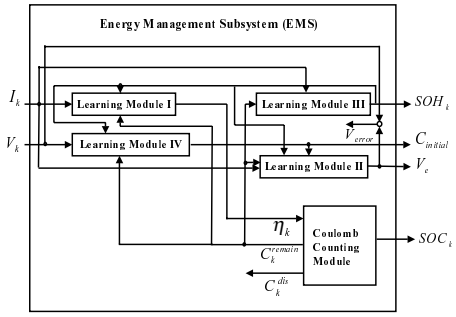

Figure 3. An illustration of the Energy Management Subsystem

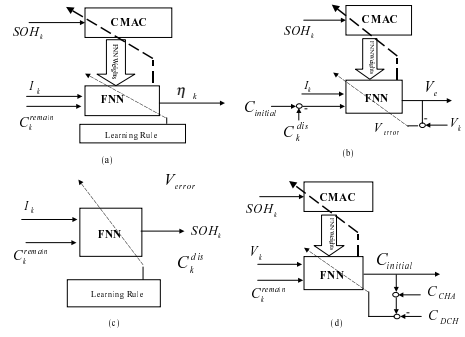

Figure 4. (a) Learning Module I (b) Learning Module II (c) Learning Module III (d) Learning Module IV

In Fig.3, system inputs are the battery voltage V_k and the discharge current I_k. The Learning Module I (LM I) represents the nonlinear mapping between the discharge current, relative remaining capacity C_k^{remain}, SOH, and battery discharge efficiency η_{I_k}. This module will send discharge efficiency η_{I_k} to the Coulomb Counting Module (CCM), and the relative battery capacities at kth and $(k-1)$st sampling times respectively can be expressed as

$$C_{I_k}^{dis} = \frac{\eta_{I_k}}{\eta_{I_{k-1}}} C_{I_{k-1}}^{dis} + I_k \Delta T \tag{5}$$

$$C_{I_1}^{dis} = I_1 \Delta T \tag{6}$$

where ΔT is the sampling time, and $C_{I_k}^{dis}$ and $C_{I_{k-1}}^{dis}$ are capacities released from the battery at kth and $(k-1)$st sampling times respectively . Thus, the SOC at the kth sampling time can be expressed as

$$SOC_k(\%) = 100 \left(1 - \frac{C_{I_k}^{dis}}{C_0} \right) \tag{7}$$

where C_0 is the battery rated capacity. The CCM implemented by Eq.(5)-(7) is also the feedback signal provider to LM I. The Learning Module II (LM II) represents the nonlinear mapping between I_k, C_k^{dis}, SOH, and V_k. The difference V_{error} will be used to update weights of FNNs and CMACs in this module. The learning rule for LM II is designed as

$$E = \frac{1}{2}(V_k - V_e)^2 \tag{8}$$

So the amount of updating weights of FNN can be expressed as

$$\Delta W_{FNN} = \frac{\partial E}{\partial W_{FNN}} \tag{9}$$

$$= (V_e - V_k) \frac{\partial V_e}{\partial W_{FNN}} \tag{10}$$

$$\tag{11}$$

Meanwhile, the learning rule for LM I can be designed as

$$\Delta W_{FNN} = \frac{\partial E}{\partial W_{FNN}} \tag{12}$$

$$= \left(\frac{\partial E}{\partial V_e} \right) \left(\frac{\partial V_e}{\partial {C_k}^{dis}} \right) \left(\frac{\partial {C_k}^{dis}}{\partial \eta_k} \right) \left(\frac{\partial \eta_k}{\partial W_{FNN}} \right) \tag{13}$$

$$= (V_e - V_k) \left(\frac{\partial V_e}{\partial {C_k}^{dis}} \right) \left(\frac{{C_{k-1}}^{dis}}{\eta_{k-1}} \right) \left(\frac{\partial \eta_k}{\partial W_{FNN}} \right) \tag{14}$$

The Learning Module III represents the nonlinear mapping between I_k, C_k^{remain}, and SOH. Its output is the estimated SOH, and the desired SOH at the kth sampling time is designed as

$$SOH_k^d(\%) = 100 \left(\frac{\eta_k}{\eta_{k-1}} \right) \tag{15}$$

The Learning Module IV represents the mapping between V_k, C_k^{remain}, SOH, and initial capacity $C_{initial}$. This module is used to estimate the remaining capacity when the rider turns on the scooter. The desired $C_{initial}$ is designed as

$$C_{initial} = C_0 - C_{k*}^{dis} \tag{16}$$

where C_{k*}^{dis} is the relative released capacity when the scooter is turned off.

The structure of combination of an FNN and a CMAC network is used to implement learning modules shown in Fig.4(a),(b), and(d). In these modules, the CMAC network will send a set of weights to the corresponding FNN according to its input. Then the FNN starts sending output signals. The learning process of the FNN begins and the updated weights of FNN are used as training patterns for the CMAC. So every learning process of learning modules includes FNN learning, CMAC learning, and their interactive learning. This kind of learning structure can enlarge the learning space coverage on complex dynamic systems[13] so as to increase the speed of convergence of learning modules used in the battery management applications.

By using learning modules, the EMS can update parameters by itself with the change of dynamics of the battery. This design avoids the unprecision resulted from the direct estimation of battery dynamics, and can govern the battery discharge characteristics much better than the method of linearly modifying SOC according to a fixed parameter model.

3 Experiment

Two parts of this experiment are described in the following sections. One is for DCS, and another is for EMS.

3.1 Testing for DCS

We used a commercially available electric scooter to conduct our experiment and road tests. A notebook computer was used to implement the intelligent control system. All the software code was written in C++ by using Borland C++ Builder 5.0, and the control signal calculated by the proposed control law was sent to the motor via the connection circuit and a DAQ card. The scooter for the experiment is shown in Fig.5(a). A rider performed the road test

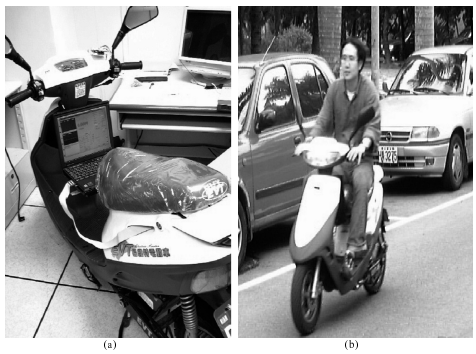

Figure 5. (a) The electric scooter for the experiment (b) Road test

according to conditions of our setup. We tested the acceleration property first. The rider would accelerate the scooter from stop to a speed at 40 km/hr with open-loop control, and this process was repeated by using the muscle-like control. The results obtained are shown in Fig.6. In Fig.6(a), the difference of speed rising times between the open-loop control and muscle-like control is about 1.5 seconds, and the rider feels no significant difference between these two control modes. Fig.6(b) shows that the muscle-like control saves about 30 % electric energy. In the second step,

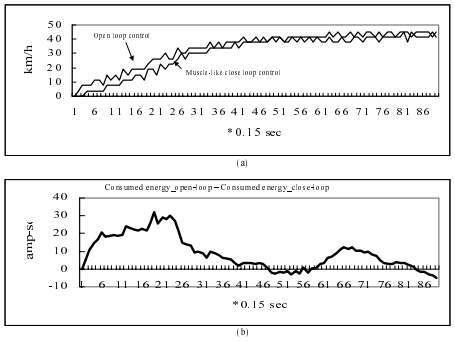

Figure 6. (a)Scooter speed under two control modes (b)Energy consumption difference under two control modes

the rider drove the scooter to slide down from a slope, starting at a point marked with x in Fig.7. When it entered a flat, its speed was reduced to 10 km/hr. Then, the rider set the desired speed at 20 Km/hr at a point marked with y in Fig.7. At the point marked z in Fig.7, the scooter climbed another slope. The current flowing into the motor increased, which reflects that controller intends to maintain the speed of the scooter. This demonstrates the muscle-like controller's capability of adapting to road conditions automatically.

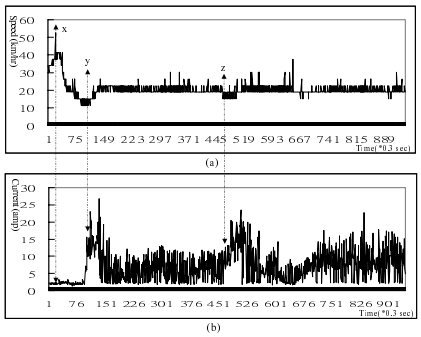

Figure 7. Change of Road Condition Test

The final test was first performed by a rider with weight 65 kg. He accelerated the scooter from stop to a speed at 30 km/hr. Then this process was repeated, with another passenger weighing 71 kg traveling together. In Fig.8, the speed rising time is shown to have a delay of 2.1 second when the total payload is 136 kg. This case demonstrates that the muscle-like controller is insensitive to the load of the scooter.

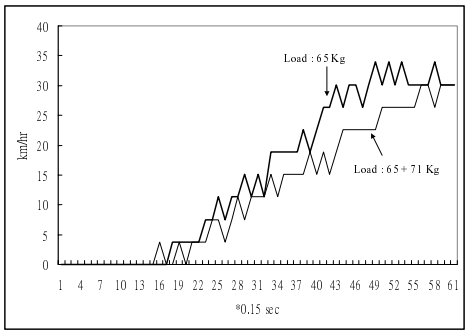

Figure 8. Results of Speed Response to Varying Loads

3.2 Testing for EMS

According to the motorcycle driving patterns estiblished by the Bureau of Standards of Ministry of Economic Affairs of Taiwan, a power consumption curve can be estimated, and it is shown in Fig.9. The battery was discharged ac-

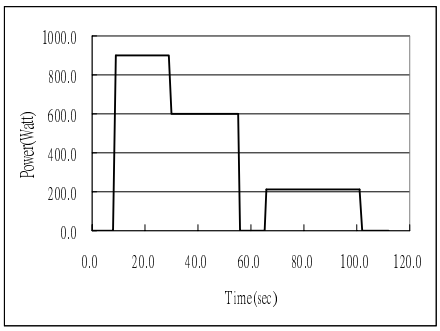

Figure 9. Power Consumption Curve

cording to this curve repeatedly until the battery voltage dropped under the cutoff voltage, 10.25V. We then charged this battery to its stantard voltage 13.2V. The discharge and charge process is called a testing cycle. We repeated the testing cycle, and checked how the EMS performed. The battery under test is a sealed lead-acid battery with a rating of 12V open-circuit voltage and 50Ah capacity, manufactured by Long Battery Co. The programmable system used to perform testing cycles is manufactured by DIGATRON

Co., and the charge and discharge currents provided range between 0A and 200A. The EMS was implemented in the same way as the DCS. Initial weights of all learning modules were trained by using 98 data sets of constant current discharge process. Every data set included a time history of battery voltage, discharge current, discharge efficiency, and capacity.

Fig. 10(a) shows the relative SOC predicted by our proposed EMS and SOC which computed by using ampere hour accumulation method at the 1st testing cycle. At the

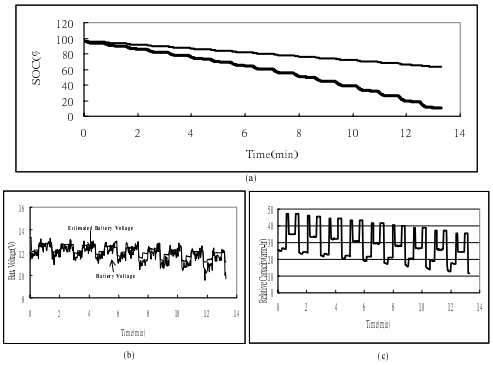

Figure 10. (a) The battery SOC predicted by EMS and ampere hour accumulation method at the 1st testing cycle (b)The sensed battery voltage and voltage predicted by EMS (c)The relative battery capacity predicted by EMS

first testing cycle, all learning modules started to learn the battery dynamics, and the learning rate is set to be 0.005 for all modules. Fig. 10(c) shows that the battery cutoff voltage is reached after 10 discharge patterns are executed. Fig. 10(a) and (b) shows that the SOC prediction error of EMS is 10 % at the end of testing, and we can see that the SOC predicted by using ampere hour accumulation method is 80 %. Therefore, the relative SOC shown in Fig.10(a) is used for checking whether the scooter speed is suitable to drive its DC motor. The estimated discharge efficiency determines the precision of relative SOC. Fig.11 shows the SOC predicted at the 20th testing cycle. The EMS prediction error is reduced to 7%, but the error for using ampere hour accumulation method is still 80%.

Fig.12(a) shows the sensed and predicted battery voltage. When we discharged the battery according to the discharge current pattern shown in Fig.12(b), we obtained the relative SOC estimation result shown in Fig.12(c). We can see that the SOC curve is almost a monotonically decreasing curve, and this property suggests that a reliable battery capacity information can be provided to the rider.

4 Conclusion

We have proposed an integrated intelligent control system for improving the performance of present electric scooters. This system utilizes a non-linear damping compliant

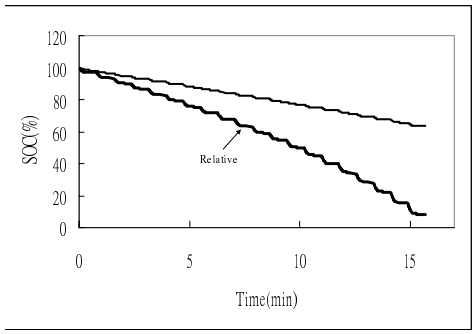

Figure 11. The battery SOC predicted by EMS and ampere hour accumulation method at the 20th testing cycle

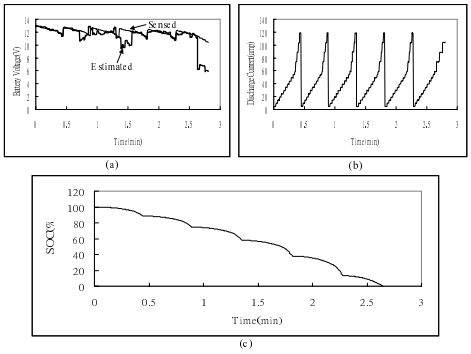

Figure 12. (a) The sensed and predicted battery voltage (b) The discharge current pattern (c) The relative SOC

control technique to provide a closed-loop control of the speed the electric scooter. It provides the rider with cruise-control capability. It also contains a battery energy management subsystem to monitor the power consumption of the battery. The energy management subsystem provides to the rider important information regarding the residual battery power of the electric scooter in terms of traveling distance, and maximum allowable traveling speed to guarantee safety arrival at the destination.

The proposed intelligent control system has greatly improved the performance of present electric scooters. Additional safety features, such as range sensors, can also be added to detect obstacles in the pathway of the electric scooter to avoid collision. For instance, the speed of the electric scooter can be reduced automatically by the system and an alarm may be turned on to alert the rider when such obstacles are detected.

References

[1] M.J. Schwarz and J.W. Shiller, Clean air act amendments of 1990, impact on motor vehicle and the environment, in *Proceedings of Air & Waste Management Association 84th Meeting Exhibition*, pp. 16–21, 1991.

[2] C.H. Wu, K. S. Hwang, and S. Lehman, Analysis and implementation of a neuromuscular-like control for robotic compliance, *IEEE Transactions on Control Systems Technology*, vol. 5, no. 6, pp. 586–597, 1997.

[3] C.T. Lin and C.S.G. Lee, Reinforcement structure/parameter learning for neural-network-based fuzzy logic control systems, *IEEE Trans. Fuzzy Syst.*, vol. 2, no. 1, pp. 46–63, 1994.

[4] J.S. Albus, A new approach to manipulator control: the cerebellar model articulation controller (CMAC), *ASME J. Dynamic Syst., Measurement, Contr.*, vol. 97, no. 3, pp. 220–227, 1975.

[5] J.S. Albus, Data storage in the cerebellar model articulation controller (CMAC), *ASME J. Dynamic Syst., Measurement, Contr.*, vol. 97, no. 3, pp. 228–233, 1975.

[6] C.H. Wu, K. Y. Young, and J. C. Houk, A neuromuscular-like model for robotic compliance control, in *Proc. of 1990 IEEE Int. Conf. On Robotics and Automation*, 1990, pp. 1885–1890.

[7] C.H. Wu, K. Y. Young, K. S. Hwang, and S. Lehman, Analysis of voluntary movements for robotic control, *IEEE Control Systems Magazine*, vol. 2, no. 1, pp. 8–14, 1992.

[8] C.H. Wu and S. L. Chang, Implementation of a neuromuscular-like control for compliance on a puma 560 robot, in *Proceedings of the 34th IEEE 1995 International Conference on Decision and Control*, 1995, pp. 1597–1602.

[9] C.H. Wu, S. L. Chang, and D. T. Lee, A study of neuromuscular-like control for rehabilitation robots, in *Proceedings of the 1996 IEEE International Conference on Robotics and Automation*, 1996, pp. 1178–1183.

[10] C. Alippi, A. Ferrero, and V. Piuri, Artificial intelligence for instruments and measurement applications, *IEEE Instrumentation & Measurement Magazine*, vol. 12, pp. 9–17, 1998.

[11] P.D. Wasserman, *Neural Computing–Theory and Practice*, Van Nostrand Reinhold, NewYork, 1989.

[12] H.J. Zimmermann, *Fuzzy Set Theory and Its Applications*, MA: Kluwer, Norwell, 3rd edition, 1996.

[13] K.Y. Young and S.J. Shiah, An approach to enlarge learning space coverage for robot learning control, *IEEE Trans. Fuzzy Syst.*, vol. 5, no. 4, pp. 511–522, 1997.

[14] P. Finger Eugene and N. Y. Brewsler, Battery of charge metering method and apparatus, *U.S. Patent*, , no. 4560937, 1985.

[15] Simmonds et al., Device for indicating the residual capacity of secondary cells, *U.S. Patent*, , no. 5479085, 1995.

[16] Kopmann, Method of and apparatus for monitoring the state of a rechargeable battery, *U.S. Patent*, , no. 5518835, 1996.

[17] Kozaki, Remaining battery capacity meter and method for computing remaining capacity, *U.S. Patent*, , no. 5691078, 1997.

[18] A.S. Clegg and C. England, Battery monitor which indicates remaining capacity by continuously monitoring instantaneous power consumption relative by expected hyperbolic discharge rates, *U.S. Patent*, , no. 5394089, 1997.

[19] F. Huet, A review of impedance measurements for determination of the state of charge or state of health of secondary batteries, *J. Power Sources*, vol. 70, pp. 59–69, 1998.